PHYSICAL REVIEW D **79,** 084012 (2009)

# Algebraic classification of numerical spacetimes and black-hole-binary remnants

Manuela Campanelli, Carlos O. Lousto, and Yosef Zlochower

*Center for Computational Relativity and Gravitation, and School of Mathematical Sciences, Rochester Institute of Technology, 78 Lomb Memorial Drive, Rochester, New York 14623, USA*

(Received 18 November 2008; published 8 April 2009)

In this paper we develop a technique for determining the algebraic classification of a numerically generated spacetime, possibly resulting from a generic black-hole-binary merger, using the Newman-Penrose Weyl scalars. We demonstrate these techniques for a test case involving a close binary with arbitrarily oriented spins and unequal masses. We find that, postmerger, the spacetime quickly approaches Petrov type II, and only approaches type D on much longer time scales. These techniques, in combination with techniques for evaluating acceleration and Newman-Unti-Tamburino parameters, allow us to begin to explore the validity of the ''no-hair theorem'' for generic merging-black-hole spacetimes.

DOI: 10.1103/PhysRevD.79.084012 PACS numbers: 04.70.Bw, 04.25.Nx, 04.30.Db

## I. INTRODUCTION

The recent breakthroughs in numerical relativity [1–3] that allowed for stable evolutions of black-hole-binary spacetimes led to many advancements in our understanding of black-hole physics, and it is now possible to accurately simulate the merger process and examine its effects in this highly nonlinear regime [4–18]. Black-hole binaries radiate between 2% and 8% of their total mass and up to 40% of their angular momenta in the last few orbits, depending on the magnitude and direction of the spin components, during the merger [4–6] (ultrarelativistic head-on black-hole mergers can radiate up to $\sim$14% of their mass [19]). In addition, the radiation of net linear momentum by a black-hole binary leads to the recoil of the final remnant hole [20–43], which can have astrophysically observable important effects [20,42,42,44–53] and represents a possible strong-field test of general relativity (GR).

In addition to important astrophysical applications, the two-body problem in GR is intrinsically interesting because it provides the framework for analyzing the behavior of the theory in the highly nonlinear, highly dynamical, nonsymmetrical regime. For example, the cosmic censorship hypothesis, that states that singularities in the universe should be cloaked by a horizon, is under active investigation [4–6,54,55]. In this paper we are interested in verifying the ''no-hair theorem,'' which states that all black holes eventually relax into a state that can be described by three parameters: the mass, spin, and charge. Hence, the final merger remnants from astrophysical multi-black-hole mergers [56,57] should be Kerr black holes [58].

The problem of determining the geometry of the final stage of a black-hole binary merger arises as a practical question in perturbative techniques, such as in the Lazarus approach [59,60], which used a combined numerical and perturbative approach to simulate the waveforms from a binary merger. In the context of the Lazarus approach, it is crucial to determine when the transition from numerical to perturbative evolutions is possible, i.e. when the full numerical simulation could be approximated by (relatively small) perturbations of a Kerr-rotating black hole, and a diagnostic, the $S$ invariant [61]

$$S = 27J^2/I^3, \tag{1}$$

that is identically 1 for a Kerr spacetime, was developed to measure the closeness of the spacetime to an algebraically special type II. However, the $S$ invariant by itself is not sufficient to demonstrate that the spacetime is near Kerr because it does not distinguish between type II and type D spacetimes, nor does it imply that the acceleration and Newman-Unti-Tamburino (NUT) parameters vanish.

More recently, with the availability of new long term evolutions, one of the consistency tests performed is the agreement of the total angular momentum of the remnant system when computed in three different ways: by measuring the angular momentum (and mass) of the remnant black hole [5,6,22] using the isolated horizon formulas [62], by measuring the total energy and angular momentum radiated [63,64] and subtracting it from the total initial values, and by looking at the quasinormal frequencies of the late-time waveforms and associate them with those of a rotating Kerr hole with mass $M$ and angular momentum per mass $a$ [23]. The rough agreement of those values represents indirect evidence that the final black hole is of the Kerr type. Furthermore, in Ref. [65], where the authors of that paper presented very-high-accuracy waveforms from the merger of an equal-mass black-hole binary, it was shown that the minimum and maximum values of the scalar curvature on the remnant horizon agreed with the Kerr values.

No-hair theorems assume a stationary Killing vector [58] as characterizations of the Kerr geometry [66,67]. While one can classify spacetimes based on their symmetry properties, here we will use a classification method based on the algebraic properties of generic spacetimes without *a priori* assumptions about symmetries.

Demonstrating that the remnant of a black-hole merger approaches Kerr asymptotically (in time) would also help

 

answer open questions about the stability of Kerr under arbitrary perturbations. The stability of the Kerr spacetime under linear perturbations has only been proven mode by mode [68], and the interior of the hole may even be unstable [69]. Hence a study of the invariant geometrical properties of the black-hole merger, which would yield a highly nontrivial perturbation of the ''Kerr'' background, may answer many open questions.

## II. MATHEMATICAL TECHNIQUES

In the following sections we will use the convention that Latin indices range over the spatial coordinates [i.e. $a = (1, 2, 3)$] and Greek indices range over all four coordinates.

### A. Petrov type

The Petrov classification of a generic spacetime is related to the number of distinct principal null directions (PNDs) of the Weyl tensor. A generic spacetime will have four linearly independent null vectors $k^\mu$ (i.e. PNDs) at all points that satisfy

$$k^\nu k^\rho k_{[\tau} C_{\mu]\nu\rho[\sigma} k_{\chi]} = 0. \tag{2}$$

Type I spacetimes have four distinct PNDs, type II have three distinct PNDs (one pair of identical PNDs and two distinct PNDs), type III have two distinct PNDs with one PND of multiplicity three, type D spacetimes have two distinct PNDs consisting of two pairs of PNDs of multiplicity two, type N spacetimes have a single PND of multiplicity four, and type O spacetimes have $C_{\mu\nu\rho\sigma} = 0$.

If the tetrad is chosen such that $l^a$ is a PND, then the Weyl scalar $\psi_0 = C_{\mu\nu\rho\sigma} l^\mu m^\nu l^\rho m^\sigma$ vanishes, and similarly, if $\psi_0 = 0$, then $l^a$ is a PND. Hence the algebraic classification of the spacetime can be obtained by finding the number of distinct choices of $l^a$ for which $\psi_0 = 0$. This amounts to finding the roots (and multiplicity of the roots) of the quartic equation [see Ref. [70], Eq. (9.5)]

$$\psi_0 + 4\lambda\psi_1 + 6\lambda^2\psi_2 + 4\lambda^3\psi_3 + \lambda^4\psi_4 = 0, \tag{3}$$

where $\psi_0, \ldots, \psi_4$ are the Weyl scalars in an arbitrary tetrad, restricted only by the condition $\psi_4 \neq 0$. This is equivalent to finding a tetrad rotation such that $\psi_0 = 0$, and if the root is repeated, then in this tetrad, $\psi_1 = 0$ (similarly if the multiplicity of the root is 3 or 4, then $\psi_2 = 0$ and $\psi_3 = 0$, respectively). If, as in type D spacetimes, there are two pairs of repeated PNDs, then we can choose a tetrad where the only nonvanishing Weyl scalar is $\psi_2$. It is important to note that the algebraic classification is done pointwise. A spacetime, as a whole, is of a particular type, if at every point the algebraic classification is of that type.

In order to determine if the numerical spacetime is algebraically special (within the numerical errors) we follow [70,71], Chap. 4. We start by defining the scalar invariants [72]

$$I = \tfrac{1}{2}\tilde{C}_{\alpha\beta\gamma\delta}\tilde{C}^{\alpha\beta\gamma\delta} \quad \text{and} \quad J = -\tfrac{1}{6}\tilde{C}_{\alpha\beta\gamma\delta}\tilde{C}^{\gamma\delta}{}_{\mu\nu}\tilde{C}^{\mu\nu\alpha\beta}, \tag{4}$$

where $\tilde{C}_{\alpha\beta\gamma\delta} = \frac{1}{4}(C_{\alpha\beta\gamma\delta} + \frac{i}{2}\epsilon_{\alpha\beta\mu\nu}C^{\mu\nu}{}_{\gamma\delta})$ (i.e. 1/2 the conjugate of the self-dual part of the Weyl tensor $C_{\alpha\beta\gamma\delta}$).

If a spacetime has repeated principal null directions, it is algebraically special. If this is the case, Eq. (3) has at least two repeated roots. In any case, Eq. (3) can be transformed into a depressed quartic [see Eq. (9) below] that, in turn, can be converted into a depressed nested cubic with roots $y$, which satisfy the condition

$$y^3 - Iy + 2J = 0. \tag{5}$$

Algebraic specialty then implies

$$I^3 = 27J^2, \tag{6}$$

i.e. $S = 1$ in Eq. (1). For types II and D the invariants $I$ and $J$ are nontrivial, while for types III, N, and O they vanish identically.

For practical applications, it is convenient to write the invariants in terms of Weyl scalars in an arbitrary null tetrad

$$I = 3\psi_2{}^2 - 4\psi_1\psi_3 + \psi_4\psi_0, \tag{7}$$

$$J = -\psi_2^3 + \psi_0\psi_4\psi_2 + 2\psi_1\psi_3\psi_2 - \psi_4\psi_1^2 - \psi_0\psi_3^2. \tag{8}$$

In order to completely determine the algebraic type we reduce Eq. (3), by changing to the variable $x = \lambda\psi_4 + \psi_3$ [73], to the form

$$x^4 + 6Lx^2 + 4Kx + N = 0, \tag{9}$$

where

$$K = \psi_1\psi_4^2 - 3\psi_4\psi_3\psi_2 + 2\psi_3^3, \tag{10}$$

$$L = \psi_2\psi_4 - \psi_3^2, \tag{11}$$

$$\begin{aligned} N &= \psi_4^2 I - 3L^2 \\ &= \psi_4{}^3\psi_0 - 4\psi_4{}^2\psi_1\psi_3 + 6\psi_4\psi_2\psi_3{}^2 - 3\psi_3{}^4 \end{aligned} \tag{12}$$

(note the typo in the definition of $N$ in Refs. [70,71]). For a type II spacetime, $K \neq 0$ and $N - 9L^2 \neq 0$, while for type D and III spacetimes, $K = 0$ and $N - 9L^2 = 0$ with $N \neq 0$. For a type N spacetime, $K = 0$ and $L = 0$ (hence $N = 0$).

Note that the above scalar objects are not invariant under arbitrary tetrad rotations [see Ref. [74], Chap. 1, Eqs. (342) [note typo there], (346) and (347)]. Tetrad rotations are classified as type I, II, and III, and have the form

$$\begin{aligned} &l^\mu \to l^\mu, \qquad n^\mu \to n^\mu + \bar{a}m^\mu + a\bar{m}^\mu + a\bar{a}l^\mu, \\ &m^\mu \to m^\mu + al^\mu, \qquad \bar{m}^\mu \to \bar{m}^\mu + \bar{a}l^\mu, \end{aligned} \tag{13}$$

$$l^\mu \to l^\mu + \bar{b}m^\mu + b\bar{m}^\mu + b\bar{b}n^\mu, \qquad n^\mu \to n^\mu,$$
$$m^\mu \to m^\mu + bn^\mu, \qquad \bar{m}^\mu \to \bar{m}^\mu + \bar{b}n^\mu, \tag{14}$$

$$l^\mu \to A^{-1}l^\mu, \qquad n^\mu \to An^\mu,$$
$$m^\mu \to e^{i\theta}m^\mu, \qquad \bar{m}^\mu \to e^{-i\theta}\bar{m}^\mu, \tag{15}$$

for type I, II, and III, respectively, where $a$ and $b$ are complex scalars and $A$ and $\theta$ are real scalars. Under these rotations the scalars $L$, $K$, and $N$ transform as

$$L \to A^2 e^{-2I\theta}L, \qquad K \to A^3 e^{-3I\theta}K, \qquad N \to A^4 e^{-4I\theta}N \tag{16}$$

for type III rotations and

$$L \to L, \qquad K \to K, \qquad N \to N \tag{17}$$

for type II rotations. Expressions for type I rotations do not have these simple forms, but we verified that, if as in type D solutions, $K = 0$ and $N - 9L^2 = 0$ in the original tetrad, then $K = 0$ and $N - 9L^2 = 0$ in the new rotated tetrad (this is also obvious for type III and II transformations above). On the other hand, $L = 0$ is not preserved by type I rotations.

Coming back to the roots $x_1$, $x_2$, $x_3$, and $x_4$ of Eq. (9), we observe that, in numerically generated spacetimes, the roots never agree exactly, even if the metric is expected to be of a special algebraic type. Of course, the root differences in each pair should scale with resolution and asymptotically approach zero as $h \to 0$ and $t \to \infty$ (where $h$ is the grid spacing).

The roots of Eq. (3) can be obtained from the roots of Eq. (5) using the following algorithm [75]:

$$\begin{aligned} D &= J^2 - (I/3)^3, \\ A &= (-J + \sqrt{D})^{1/3}, \\ B &= (-J - \sqrt{D})^{1/3}, \\ y_1 &= A + B, \\ y_2 &= -\frac{1}{2}(A + B) + i\frac{\sqrt{3}}{2}(A - B), \\ y_3 &= -\frac{1}{2}(A + B) - i\frac{\sqrt{3}}{2}(A - B), \end{aligned} \tag{18}$$

where the complex phases of $A$ and $B$ are chosen such that $AB = I/3$. The roots of Eq. (9) are then obtained from the roots of the complete cubic equation for the variable $z$ (where $z = 2\psi_4 y - 4L$)

$$z^3 + 12Lz^2 + 4(9L^2 - N)z - 16K = 0, \tag{19}$$

which has the roots

$$z_1 = 2\psi_4 y_1 - 4L, \qquad z_2 = 2\psi_4 y_2 - 4L,$$
$$z_3 = 2\psi_4 y_3 - 4L. \tag{20}$$

Finally the roots of our original equation (3) can be written in the form [73]

$$\begin{aligned} \lambda_1 &= [-\psi_3 + \tfrac{1}{2}(\sqrt{z_1} + \sqrt{z_2} + \sqrt{z_3})]/\psi_4, \\ \lambda_2 &= [-\psi_3 + \tfrac{1}{2}(\sqrt{z_1} - \sqrt{z_2} - \sqrt{z_3})]/\psi_4, \\ \lambda_3 &= [-\psi_3 + \tfrac{1}{2}(-\sqrt{z_1} + \sqrt{z_2} - \sqrt{z_3})]/\psi_4, \\ \lambda_4 &= [-\psi_3 + \tfrac{1}{2}(-\sqrt{z_1} - \sqrt{z_2} + \sqrt{z_3})]/\psi_4, \end{aligned} \tag{21}$$

where the signs of the $\sqrt{z_i}$ are chosen such that $(\sqrt{z_1}\sqrt{z_2}\sqrt{z_3}) = -4K$. We note that in a type D spacetime $\lambda_1 = \lambda_2$ and $\lambda_3 = \lambda_4$.

### B. Vacuum

The determination of the algebraic type of the matter fields can be done in an analogous way using the Ricci tensor, rather than the Weyl scalars. The analogue of the Petrov types are the Segre types and the equation to determine the multiplicities of the roots is [see [70], Eq. (9.2)]

$$\sigma^4 - \tfrac{1}{2}I_6\sigma^2 - \tfrac{1}{3}I_7\sigma + \tfrac{1}{8}(I_6^2 - 2I_8) = 0, \tag{22}$$

where

$$I_6 = S^\alpha_\beta S^\beta_\alpha, \tag{23}$$

$$I_7 = S^\alpha_\beta S^\beta_\gamma S^\gamma_\alpha, \tag{24}$$

$$I_8 = S^\alpha_\beta S^\beta_\gamma S^\gamma_\delta S^\delta_\alpha, \tag{25}$$

and

$$S_{\alpha\beta} = R_{\alpha\beta} - \tfrac{1}{4}g_{\alpha\beta}R, \tag{26}$$

is the trace free part of the Ricci tensor.

This characterization of the matter fields does not completely determine the algebraic properties, and other additional criteria have to be used. In our numerical simulations here, we are concerned with vacuum spacetimes. Numerical evolutions may introduce artificial (and unphysical) matter fields through violations of the Hamiltonian and momentum constraints, and the natural way of monitoring the accuracy of the solution is to examine these constraints and confirm that the induced matter fields converge to zero with resolution and in time.

### C. Determination of the Kerr solution

Once we determine that a solution is, for instance, Petrov type D and is a vacuum solution, we still do not uniquely single out the Kerr spacetime. One can go further and try to determine if the spacetime has the symmetries of Kerr (the Kerr spacetime has two commuting spacelike and timelike Killing vectors [76]). However, one still needs to examine the asymptotic behavior of the solutions to determine that the spacetime does not have a NUT charge $l$ or acceleration $\alpha$.

A general type D, vacuum black-hole solution can be described by the metric [see [77], Eq. (17)]

$$ds^2 = \frac{1}{\Omega^2}\left\{\frac{Q}{\rho^2}\left[dt - \left(a\sin^2\theta + 4l\sin^2\frac{\theta}{2}\right)d\phi\right]^2 - \frac{\rho^2}{Q}dr^2 - \frac{P}{\rho^2}[adt - (r^2 + (a+l)^2)d\phi]^2 - \frac{\rho^2}{P}\sin^2\theta d\theta^2\right\}, \tag{27}$$

where

$$\Omega = 1 - \alpha(l + a\cos\theta)r, \tag{28}$$

$$\rho^2 = r^2 + (l + a\cos\theta)^2, \tag{29}$$

$$P = \sin^2\theta(1 - a_3\cos\theta - a_4\cos^2\theta), \tag{30}$$

$$Q = k - 2mr + \epsilon r^2 - 2\alpha n r^3 - \alpha^2 k r^4, \tag{31}$$

and

$$a_3 = 2\alpha am - 4\alpha^2 alk, \tag{32}$$

$$a_4 = -\alpha^2 a^2 k \tag{33}$$

with $\epsilon$, $n$ and $k$ as given a function of the more basic parameters $m$, $l$, $a$, and $\alpha$ by

$$\epsilon = \frac{k}{a^2 - l^2} + 4\alpha lm - (a^2 + 3l^2)\alpha^2 k, \tag{34}$$

$$n = \frac{kl}{a^2 - l^2} - \alpha(a^2 - l^2)m + (a^2 - l^2)l\alpha^2 k, \tag{35}$$

$$\left(\frac{1}{a^2 - l^2} + 3\alpha^2 l^2\right)k = 1 + 2\alpha lm. \tag{36}$$

If the null tetrad is aligned with the principal null directions, i.e.

$$\begin{aligned} l^\mu &= \frac{(1-\alpha pr)}{\sqrt{2(r^2+p^2)}}\left[\frac{1}{\sqrt{Q}}(r^2\partial_\tau - \partial_\sigma) - \sqrt{Q}\partial_r\right], \\ n^\mu &= \frac{(1-\alpha pr)}{\sqrt{2(r^2+p^2)}}\left[\frac{1}{\sqrt{Q}}(r^2\partial_\tau - \partial_\sigma) + \sqrt{Q}\partial_r\right], \\ m^\mu &= \frac{(1-\alpha pr)}{\sqrt{2(r^2+p^2)}}\left[-\frac{1}{\sqrt{P}}(p^2\partial_\tau + \partial_\sigma) + i\sqrt{P}\partial_p\right], \end{aligned} \tag{37}$$

then the only nonvanishing Weyl scalar is

$$\Psi_2 = -(m + in)\left(\frac{1 - \alpha pr}{r + ip}\right)^3, \tag{38}$$

where $p = l + a\cos\theta$.

It is then natural to look at the asymptotic behavior of the spacetime to determine if there is a NUT charge $l$, an acceleration $\alpha$, or if the spacetime is plain Kerr. One can use the method of determining a quasi-Kinnersley frame [59,78] to compute $\psi_2$ and perform the above analysis. Alternatively, we can use the fact that, once we determined the spacetime is type D, we can choose a tetrad where all the Weyl scalars, but $\psi_2$, vanish. Hence the invariants $I$ and $J$ must have the form

$$I = 3\psi_2^2, \qquad J = -\psi_2^3 \tag{39}$$

in this special class of tetrads.

If the acceleration $\alpha \neq 0$, then a series expansion of the invariant $I$ gives

$$I = 3(m + il)^2\alpha^6 p^6 - \frac{18}{r}(m + il)^2\alpha^5 p^5(i\alpha p^2 + 1) + \mathcal{O}\left(\frac{1}{r^2}\right). \tag{40}$$

Note that if the acceleration $\alpha = 0$, then $n = l$. An asymptotic expansion of the $I$ invariant for the metric (27) then gives

$$I = \frac{3}{r^6}(m + il)^2 - \frac{18i}{r^7}(m + il)^2(l + a\cos\theta) + \mathcal{O}\left(\frac{1}{r^8}\right), \tag{41}$$

and, by looking at the real and imaginary parts of the $I$ invariant at large radii, we can determine the $l$ parameter via

$$\Im(I)/\Re(I) = \begin{cases} \frac{2ml}{m^2 - l^2}; & l \neq 0, \\ \frac{-6a\cos\theta}{r}; & l = 0. \end{cases} \tag{42}$$

We will use this method to determine the asymptotic behavior of the final remnant of a black-hole-binary merger. Note that using $I$ and $J$ only requires smooth second derivatives of the metric, which has a distinct advantage over higher-derivative methods when dealing with numerically generated spacetimes.

## III. NUMERICAL TECHNIQUES

To compute the numerical initial data, we use the puncture approach [79] along with the TWOPUNCTURES [80] code. In this approach the 3-metric on the initial slice has the form $\gamma_{ab} = (\psi_{\rm BL} + u)^4\delta_{ab}$, where $\psi_{\rm BL}$ is the Brill-Lindquist conformal factor, $\delta_{ab}$ is the Euclidean metric, and $u$ is (at least) $C^2$ on the punctures. The Brill-Lindquist conformal factor is given by $\psi_{\rm BL} = 1 + \sum_{i=1}^{n} m_i^p/(2|\vec{r} - \vec{r}_i|)$, where $n$ is the total number of "punctures", $m_i^p$ is the mass parameter of puncture $i$ ($m_i^p$ is *not* the horizon mass associated with puncture $i$), and $\vec{r}_i$ is the coordinate location of puncture $i$. We evolve these black-hole-binary data sets using the LAZEV [81] implementation of the moving puncture approach [2,3]. In our version of the moving puncture approach we replace the Baumgarte-Shapiro-Shibata-Nakamura (BSSN) [82–84] conformal exponent $\phi$, which has logarithmic singularities at the punctures, with the initially $C^4$ field $\chi = \exp(-4\phi)$. This new variable, along with the other BSSN variables, will remain finite provided that one uses a suitable choice for the

gauge. An alternative approach uses standard finite differencing of $\phi$ [3]. Recently Marronetti *et al.* [85] proposed the use of $W = \sqrt{\chi}$ as an evolution variable. For the runs presented here we use centered, eighth-order finite differencing in space [56] and a fourth-order Runge-Kutta time integrator (note that we do not upwind the advection terms).

We use the CARPET [86] mesh refinement driver to provide a ''moving boxes'' style mesh refinement. In this approach refined grids of fixed size are arranged about the coordinate centers of both holes. The CARPET code then moves these fine grids about the computational domain by following the trajectories of the two black holes.

We obtain accurate, convergent waveforms and horizon parameters by evolving this system in conjunction with a modified 1 + log lapse and a modified Gamma-driver shift condition [2,87], and an initial lapse $\alpha(t = 0) = 2/(1 + \psi_{\rm BL}^4)$. The lapse and shift are evolved with

$$(\partial_t - \beta^i \partial_i)\alpha = -2\alpha K, \tag{43a}$$

$$\partial_t \beta^a = B^a, \tag{43b}$$

$$\partial_t B^a = 3/4 \partial_t \tilde{\Gamma}^a - \eta B^a. \tag{43c}$$

These gauge conditions require careful treatment of $\chi$, the inverse of the 3-metric conformal factor, near the puncture in order for the system to remain stable [2,7,8]. As shown in Ref. [88], this choice of gauge leads to a strongly hyperbolic evolution system provided that the shift does not become too large. In our tests, $W$ showed better behavior at very early times ($t < 10M$) (i.e. did not require any special treatment near the punctures), but led to evolutions with larger truncation errors (importantly, larger orbital phase errors) when compared to $\chi$.

We use AHFINDERDIRECT [89] to locate apparent horizons. We measure the magnitude of the horizon spin using the isolated horizon algorithm detailed in [62]. This algorithm is based on finding an approximate rotational Killing vector (i.e. an approximate rotational symmetry) on the horizon $\varphi^a$. Given this approximate Killing vector $\varphi^a$, the spin magnitude is

$$S_{[\varphi]} = \frac{1}{8\pi} \oint_{\rm AH} (\varphi^a R^b K_{ab}) d^2V, \tag{44}$$

where $K_{ab}$ is the extrinsic curvature of the 3D slice, $d^2V$ is the natural volume element intrinsic to the horizon, and $R^a$ is the outward pointing unit vector normal to the horizon on the 3D slice. We measure the direction of the spin by finding the coordinate line joining the poles of this Killing vector field using the technique introduced in [6]. Our algorithm for finding the poles of the Killing vector field has an accuracy of $\sim 2°$ (see [6] for details). Note that once we have the horizon spin, we can calculate the horizon mass via the Christodoulou formula (which is exact for a Kerr black hole)

$$m^H = \sqrt{m_{\rm irr}^2 + S^2/(4m_{\rm irr}^2)}, \tag{45}$$

where $m_{\rm irr} = \sqrt{A/(16\pi)}$ and $A$ is the surface area of the horizon.

We also use an alternative quasilocal measurement of the spin and linear momentum of the individual black holes in the binary that is based on the coordinate rotation and translation vectors [22]. In this approach the spin components of the horizon are given by

$$S_{[i]} = \frac{1}{8\pi} \oint_{\rm AH} \phi^a_{[i]} R^b K_{ab} d^2V, \tag{46}$$

where $\phi^i_{[\ell]} = \delta_{\ell j}\delta_{mk} r^m \epsilon^{ijk}$, $\epsilon^{123} = 1$, and $r^m = x^m - x_0^m$ is the coordinate displacement from the centroid of the hole, while the linear momentum is given by

$$P_{[i]} = \frac{1}{8\pi} \oint_{\rm AH} \xi^a_{[i]} R^b (K_{ab} - K\gamma_{ab}) d^2V, \tag{47}$$

where $\xi^i_{[\ell]} = \delta^i_\ell$.

### A. Numerical tetrad and root finder

We calculate $\psi_0 \ldots \psi_4$ using the tetrad

$$l^\mu = (t^\mu + r^\mu)/\sqrt{2}, \tag{48}$$

$$n^\mu = (t^\mu - r^\mu)/\sqrt{2}, \tag{49}$$

$$m^\mu = (\theta^\mu + i\phi^\mu)/\sqrt{2}, \tag{50}$$

where $t^\mu$ is the unit normal to the $t =$ const slices and $\{r^\mu, \theta^\mu, \phi^m u\}$ are unit spacelike vectors (with the time component equal to zero) constructed as follows [60]. We start with the unit vector

$$\phi^a = \hat{\tilde{\phi}}^a, \tag{51}$$

where $\tilde{\phi}^a = \{-y, x, 0\}$, $\hat{v}^a = v^a/\sqrt{v^a v^b \gamma_{ab}}$, and $\gamma_{ab}$ is the spatial metric. We then find the unit vector in the radial direction perpendicular to $\phi^a$

$$r^a = \hat{\tilde{r}}^a, \tag{52}$$

where

$$\tilde{r}^a = \check{r}^a - \check{r}^a \phi^b \gamma_{ab}, \tag{53}$$

and $\check{r}^a = \{x, y, z\}$. Finally, we obtain

$$\theta^a = \hat{\tilde{\theta}}^a, \tag{54}$$

where

$$\tilde{\theta}^a = \gamma^{ab} \epsilon_{bcd} \phi^c r^d. \tag{55}$$

With this choice of tetrad $\psi_0 \ldots \psi_4$ are all nonvanishing for Kerr spacetimes when the specific spin $a$ is nonvanishing.

TABLE I. Initial data parameters for the numerical evolution. The punctures have mass parameters $m_i^p$, horizons masses $m_i^H$, momenta $\pm\vec{p}$, spins $\vec{S}_i$, and the configuration has a total Arnowitt-Deser-Misner (ADM) mass $M_{\rm ADM} = 1.000\,000\,4M$.

| | | | |
|---|---|---|---|
| $m_1^p/M$ | 0.377 52 | $m_2^p/M$ | 0.424 52 |
| $m_1^H/M$ | 0.462 98 | $m_2^H/M$ | 0.578 72 |
| $x_1/M$ | −0.750 23 | $x_2/M$ | 0.580 04 |
| $y_1/M$ | 1.116 79 | $y_2/M$ | −0.894 49 |
| $z_1/M$ | −0.160 93 | $z_2/M$ | 0.203 38 |
| $S_1^x/M^2$ | −0.020 765 | $S_2^x/M^2$ | 0.121 06 |
| $S_1^y/M^2$ | 0.065 806 | $S_2^y/M^2$ | −0.055 32 |
| $S_1^z/M^2$ | 0.054 697 | $S_2^z/M^2$ | 0.161 78 |
| $p^x/M$ | −0.134 735 | $p^y/M$ | −0.213 76 |
| $p^z/M$ | −0.012 323 | | |

### B. Initial data

To generate the initial data parameters, we used random values for the mass ratio and spins of the binary (the ranges for these parameters were chosen to make the evolution practical). We then calculated approximate quasicircular orbital parameters for a binary with these chosen parameters at an initial orbital separation of $50M$ and evolved using purely post-Newtonian evolutions until the binary separation decreased to $2.3M$. The goal was to produce a binary that had no particular symmetries, so that we can draw general conclusions from the results, while also merging very quickly (within $15M$ of the start of the simulation), to reduce the computational expense. The initial binary configuration at $r = 50M$ was chosen such that $q = m_1/m_2 = 0.8$, $\vec{S}_1/m_1^2 = (-0.2, -0.14, 0.32)$, and $\vec{S}_2/m_2^2 = (-0.09, 0.48, 0.35)$. This is the same basic configuration that we used in [90]. We summarize the initial data parameters in Table I.

## IV. RESULTS

We ran the binary configuration using 9 levels of refinement with an outer grid of resolution $h = 3.2M$ extending to $\pm 416M$. The resolution on the finest grid was $h = M/80$. We analyze the Weyl scalars in the region $r \lesssim 5M$ where we had a resolution of $h \leq M/20$. This calculation is nontrivial because the magnitudes of the Weyl scalars can be quite small (we need to analyze these scalars at very late times when the waveform amplitudes are quite small), requiring very-high overall simulation accuracy. We found that the isolated horizon formulas and the radiated energy and angular momentum both predict similar remnant masses and spins, with the isolated horizon formulas Eqs. (44)–(46) giving $M_{\rm rem} = 0.9859$, $\vec{S}_{\rm rem} = \{0.001\,60 \pm 0.000\,05, 0.0407 \pm 0.0004, 0.7173 \pm 0.0001\}$ and the radiation giving $M_{\rm rem} = 0.9861 \pm 0.0001$, $\vec{S}_{\rm rem} = \{0.001\,53 \pm 0.000\,01, 0.040\,78 \pm 0.000\,02, 0.7179 \pm 0.0001\}$. A fit to the quasinormal profile $\sim \exp(-\alpha t)\sin(\omega t)$ gives $\alpha = 0.079\,97 \pm 0.0013$ and $\omega = 0.5603 \pm 0.0025$, where the values quoted are the average from fits to the real and imaginary parts of the $(\ell = 2, m = 2)$ component of $\psi_4$ extracted at $r = 100M$ over the domain $(160M < t < 200M)$. The resulting values of $M_{\rm rem}$ and $a/M_{\rm rem}$ [91] are $0.9876 \pm 0.0079$ and $0.743 \pm 0.013$, respectively. Note that the isolated horizon and radiated energy/momentum formulas predict that the final specific spin is $a/M_{\rm rem} = 0.739\,31 \pm 0.000\,16$. This agreement is consistent with the final remnant being a Kerr hole (note that this consistency is not a proof that the remnant is Kerr).

If the spacetime is algebraically special, then the roots $y_2$ and $y_3$ of Eq. (5) are equal. To measure how far the spacetime is from being algebraically special we plot the magnitude $|(y_3 - y_2)/y_1|$ (here $y_1$ provides a natural normalization) and the invariant $S - 1$ at the point $(x = 5M, y = z = 0)$ (see Figs. 1 and 2) [59,60,92]. From the figures we can see that the deviation of the spacetime from being algebraically special decreases exponentially (with an $e$-folding time of $\sim 20M$ for $y_1 - y_2$ and $\sim 10M$ for $S - 1$) with time until $t \sim 150M$. The oscillation seen after this time may be due to reflections off of the refinement boundaries (this, in turn, provides a sensitive test to improve the numerical techniques).

In Figs. 3–7 we show the unnormalized magnitudes of the root-pair differences $|\lambda_1 - \lambda_2|$ and $|\lambda_3 - \lambda_4|$ both as a function of $t$ at a fixed $(x, y, z) = (5, 0, 0)$ and along the $x$ axis at several times. Both pairs show a general decrease in the magnitudes of the differences with time, but with a pronounced oscillatory behavior. Note that $|\lambda_1 - \lambda_2|$ separation is much smaller than the $|\lambda_3 - \lambda_4|$ separation, indicating that the spacetime first approaches type II (and hence is algebraically special with $S - 1 \sim 0$) before set-

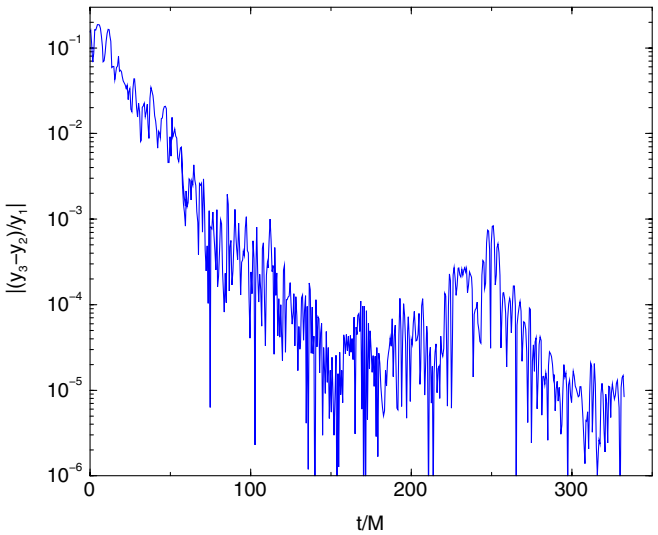


FIG. 1 (color online). The magnitude $|(y_3 - y_2)/y_1|$ versus time at the point $x = 5M$, $y = 0$, $z = 0$. The spacetime is algebraically special if $|(y_3 - y_2)/y_1| = 0$. Note the initial exponential decrease in the root difference.

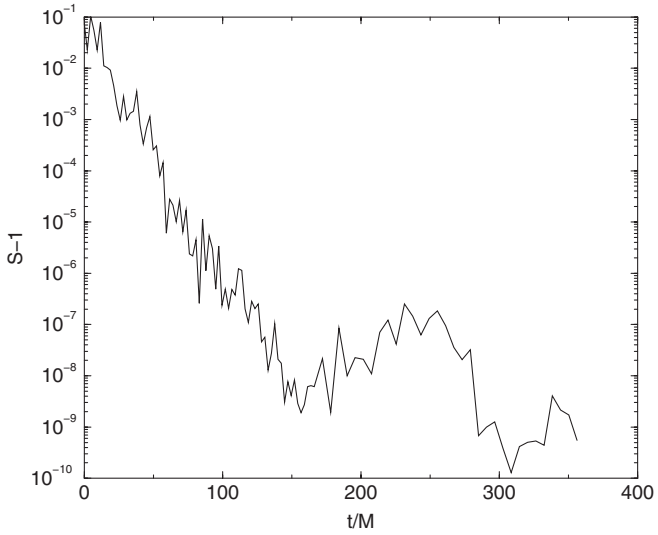


FIG. 2. The magnitude $|S-1|$ versus time at the point $x = 5M$, $y = 0$, $z = 0$. The spacetime is algebraically special if $S = 1$. Note the initial exponential decrease in $S - 1$.

tling to type D. In Fig. 8 we plot the values of the pairs $(\lambda_1, \lambda_2)$ and $(\lambda_3, \lambda_4)$ on the complex plane at the point $(5, 0, 0)$ for times $t = 57, \ldots, 166.25$ in steps of 0.593 75. From the plots we can see how each of the two roots in the root pairs approach each other. In Fig. 5 we plot the magnitude of the root separations normalized by the difference between the average value of the roots in each pair (note that $|\lambda_2 - \lambda_3|$ has an $e$-folding time of $\sim 30M$). It takes about $80M$ of evolution, or $65M$ postmerger, until the larger normalized root separation falls below 1. Finally, in Fig. 6 we show the $L_2$ norm of the root separations along the $x$ and $y$ axes restricted to $2M < |x|, |y| < 5M$ and $2M < |x|, |y| < 10M$ (the restriction to $|x|, |y| > 2M$ is

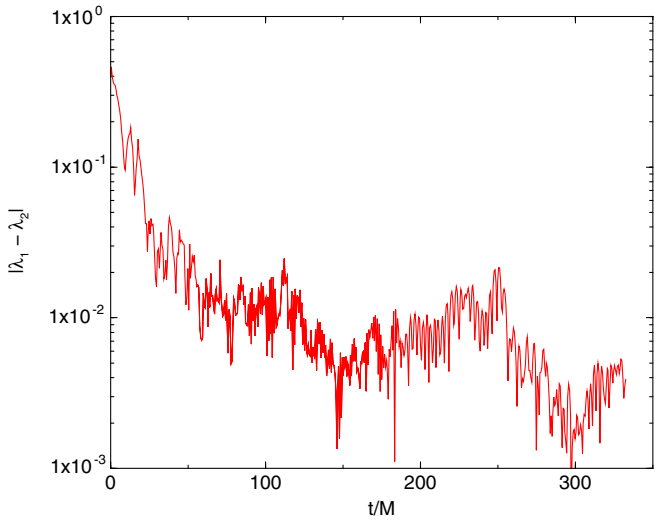


FIG. 3 (color online). The magnitude of the root-pair separation $|\lambda_1 - \lambda_2|$ versus time for the two roots close to $\lambda = 0$ at the point $x = 5M$, $y = 0$, $z = 0$.

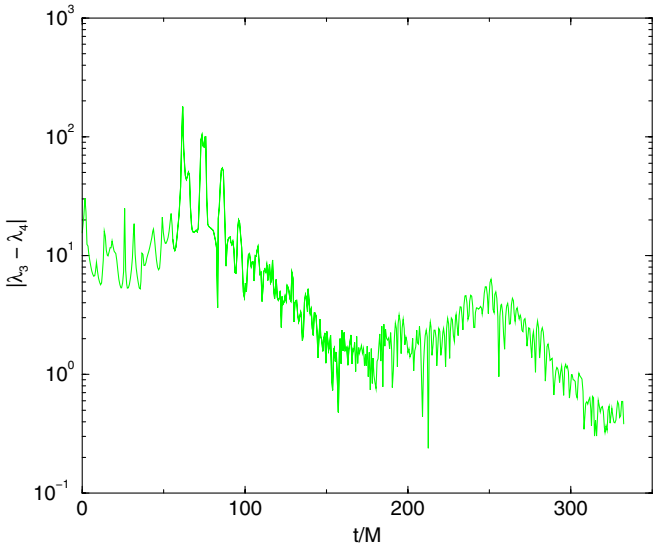


FIG. 4 (color online). The magnitude of the root-pair separation $|\lambda_3 - \lambda_4|$ versus time for the two roots furthest from $\lambda = 0$ at the point $x = 5M$, $y = 0$, $z = 0$. Note that there is no rapid decrease in the $|\lambda_3 - \lambda_4|$ which indicates that the spacetime is not approaching type D as fast as it is approaching type II.

such that the black-hole interior is not included in the norm). The poorer convergence of the norm over the larger domain is due to numerical errors in the more coarsely resolved regions.

In Fig. 9 we plot $r|I|$ versus $r/M$ along the $+y$ axis and along the line $(x = 0, y = z)$. The leading-order term if $\alpha \neq 0$ is proportional to $(\alpha p)^6$, where $p = l + a\cos\theta$ [see Eq. (27)]. If $l = 0$, then $p = a\cos\theta$, and along the $y$ axis, $p^6 \sim 10^{-9}$ (the remnant spin is slightly misaligned with

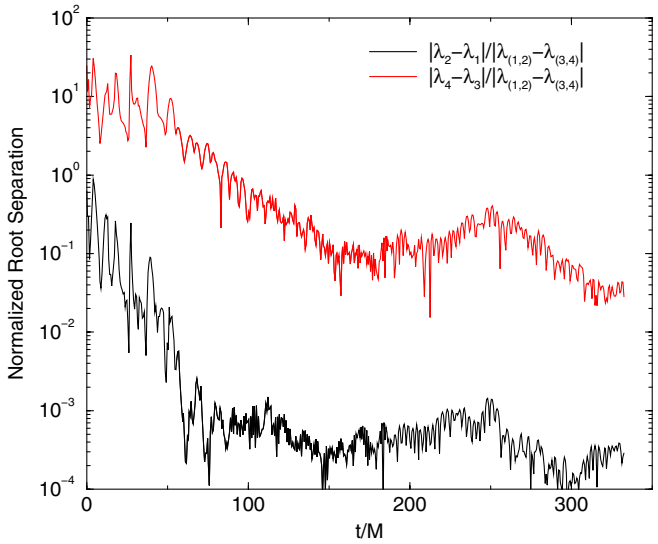


FIG. 5 (color online). The magnitude of the two root-pair separations normalized by the magnitude of the differences of the average value of the roots in each pair $|\lambda_{(1,2)} - \lambda_{(3,4)}|$, where $\lambda_{(1,2)} = (\lambda_1 + \lambda_2)/2$ and $\lambda_{(3,4)} = (\lambda_3 + \lambda_4)/2$.

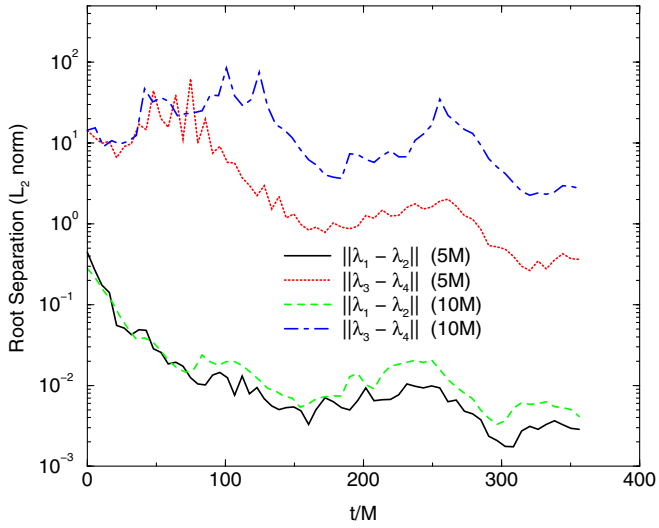


FIG. 6 (color online). The $L_2$ norm of the root separations versus time along the $x$ and $y$ axis for $2 < |x|, |y| < 5$ and $2 < |x|, |y| < 10$. The region containing the black hole itself was excluded from the norm.

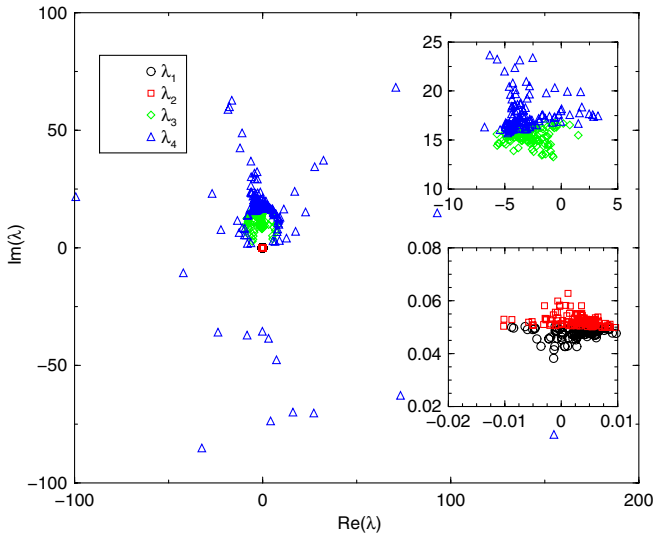


FIG. 8 (color online). The locations on the complex plane of the roots $\lambda_1, \ldots, \lambda_4$ for $t = 57, 57.593\,75, \ldots, 166.25$ at the point $(x = 5, y = 0, z = 0)$. The insets shows the last 107 points. Note that $\lambda_4$ has the largest scatter in time and that the separation of $\lambda_1$ and $\lambda_2$ is not distinguishable on the overall plot. Initially, the points at different times are scattered, but converge to a fixed limit at late times.

the $z$ axis), but along the line $(x = 0, y = z)$, $p^6 \sim 0.028$. From the data on the $y$ axis we can only conclude that $\alpha l$ is very small. However, along the diagonal, $p^6 \sim 0.028 + 0.30l$, which provides evidence that both $\alpha$ and $l$ are small. In Fig. 10 we plot the function $r\Im(I)/\Re(I)$ versus $M/x$ along the $+x$ axis for various times from $t \sim 100$ to $t \sim 350M$. It is clear from the plot that this function does not tend to $\infty$ at larger $r$, which indicates that the NUT charge of the space time vanishes (i.e. given that we already found that $\alpha$ vanishes). Hence we can see good evidence that the spacetime is approaching type D with zero NUT charge and zero acceleration, and hence is approaching a Kerr spacetime.

We have confirmed that the constraints converge to zero for our code outside of the horizons. For this simulation the constraint violations where of order $10^{-4}$ at the horizons,

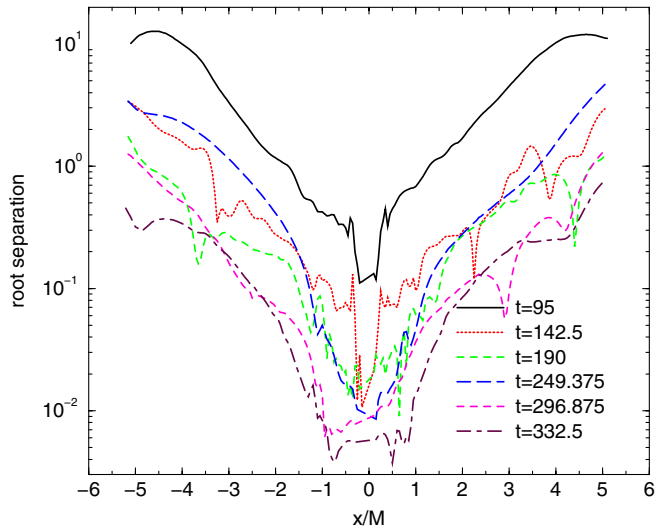


FIG. 7 (color online). The magnitude of the root-pair separation $|\lambda_3 - \lambda_4|$ along the $x$ axis for several values of $t$. At first the root separation decreases significantly with time, but eventually stabilizes as numerical errors due to reflections off the refinement boundaries and other numerical sources of error begin to dominate.

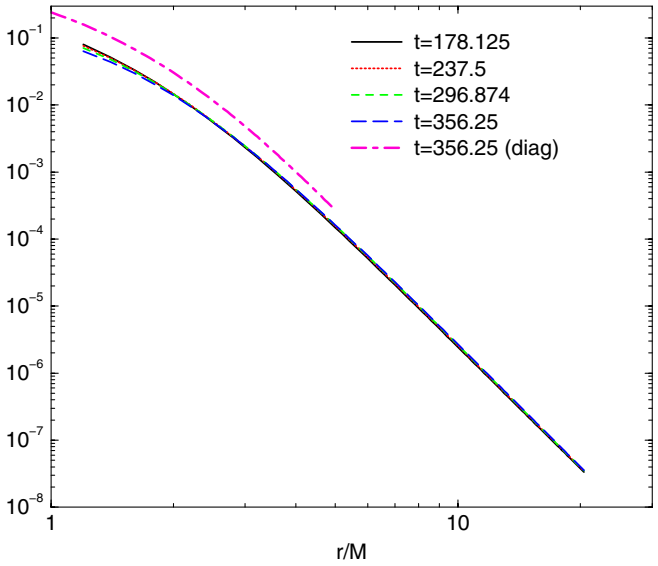


FIG. 9 (color online). $r|I|$ as a function of $r/M$ along the $y$ axis and the diagonal line $(x = 0, y = z)$. Note that the behavior indicates that $r|I| \to 0$ as $r \to \infty$, which indicates that the acceleration $\alpha$ vanishes.

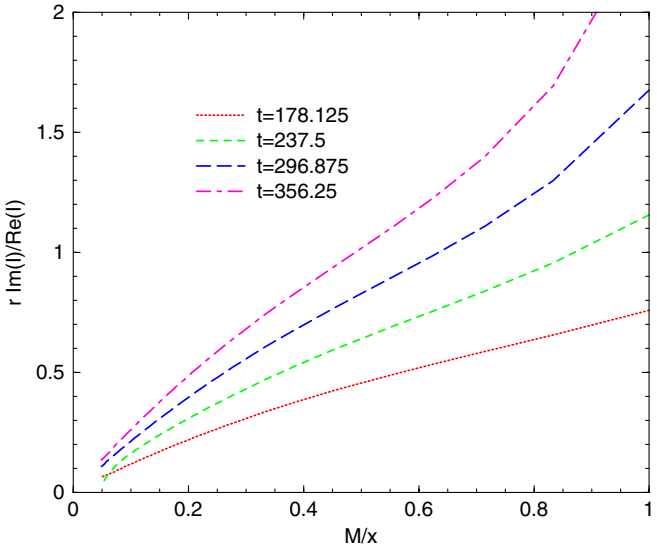


FIG. 10 (color online). The ratio $r\Im(I)/\Re(I)$ as a function of $M/x$ along the $x$ axis. Note that the behavior indicates that $\Im(I)/\Re(I) \to 0$ as $r \to \infty$ (i.e. $M/x \to 0$), which indicates that the NUT charge vanishes.

and dropped off steeply with radius. Convergence of the constraints is important to show that the spacetime remains a vacuum spacetime outside of the remnant horizons.

## V. CONCLUSION

We have provided a method to classify numerically generated spacetimes according to their algebraic properties. This is based on the use of the coincidence of the principal null directions for algebraically special spacetimes. In particular, we focus on the final remnant of a generic-black-hole-binary merger, that, according to the no-hair theorem, is expected to produce a Kerr black hole, and hence be of algebraic (Petrov) type D (i.e. that the four principal null directions agree in pairs). We give a measure of the agreement by normalizing the numerical differences between two nearby roots of Eq. (3) with the average separation to the other root pair in the complex plane.

We have been able to verify this agreement to order $10^{-4}$ and $10^{-2}$ for the two pairs, respectively. We find that the agreement of the two roots in each pair improves with evolution time and only appears to be limited by unphysical boundary effects (from the refinement and outer boundaries). The late-time behavior of these two root pairs implies that the spacetime near the remnant first approaches an algebraically special type II (with one pair of roots and two distinct roots) and over longer time scales approaches type D. We also analyze the invariant asymptotic behavior of the spacetime and do not find evidence for nonzero acceleration or NUT parameters. Thus, our simulations would suggest that the spacetime indeed approaches Kerr, which incidentally, is also a strong test of the stability of the Kerr solution under large, generic perturbations within the time scales of the simulation.

These results represent the first such tests for generic binary mergers using modest computational resources. This naturally suggests that further studies, perhaps also involving other numerical evolution methods, such as pseudospectral [93,94] and multipatch, multiblock [95,96], be used to test the algebraic structure of the remnants of binary mergers. Finally, the algebraic structure of the remnants from the merger of more than two black holes (e.g. close encounters [56,57] of multiple black holes), while expected to have the same structure as the remnants of binaries, could conceivably have different algebraic structures. Thus it would be interesting to use these techniques to examine those remnants.

## ACKNOWLEDGMENTS

We thank S. Dain for insightful comments and M. Mars for bringing the C-metric to our attention. We gratefully acknowledge NSF for financial support from Grants No. PHY-0722315, No. PHY-0653303, No. PHY 0714388, and No. PHY 0722703 and NASA for financial support from Grants No. NASA 07-ATFP07-0158 and No. HST-AR-11763.01. Computational resources were provided by Lonestar cluster at TACC and by NewHorizons at RIT.

[1] F. Pretorius, Phys. Rev. Lett. **95**, 121101 (2005).
[2] M. Campanelli, C. O. Lousto, P. Marronetti, and Y. Zlochower, Phys. Rev. Lett. **96**, 111101 (2006).
[3] J. G. Baker, J. Centrella, D.-I. Choi, M. Koppitz, and J. van Meter, Phys. Rev. Lett. **96**, 111102 (2006).
[4] M. Campanelli, C. O. Lousto, and Y. Zlochower, Phys. Rev. D **74**, 041501(R) (2006).
[5] M. Campanelli, C. O. Lousto, and Y. Zlochower, Phys. Rev. D **74**, 084023 (2006).
[6] M. Campanelli, C. O. Lousto, Y. Zlochower, B. Krishnan, and D. Merritt, Phys. Rev. D **75**, 064030 (2007).
[7] M. Campanelli, C. O. Lousto, and Y. Zlochower, Phys. Rev. D **73**, 061501(R) (2006).
[8] B. Brugmann *et al.*, Phys. Rev. D **77**, 024027 (2008).
[9] J. G. Baker, J. Centrella, D.-I. Choi, M. Koppitz, and J. van Meter, Phys. Rev. D **73**, 104002 (2006).
[10] F. Pretorius, Classical Quantum Gravity **23**, S529 (2006).

[11] F. Pretorius and D. Khurana, Classical Quantum Gravity **24**, S83 (2007).
[12] J. G. Baker, J. R. van Meter, S. T. McWilliams, J. Centrella, and B. J. Kelly, Phys. Rev. Lett. **99**, 181101 (2007).
[13] A. Buonanno, G. B. Cook, and F. Pretorius, Phys. Rev. D **75**, 124018 (2007).
[14] J. G. Baker *et al.*, Phys. Rev. D **75**, 124024 (2007).
[15] M. A. Scheel *et al.*, Phys. Rev. D **74**, 104006 (2006).
[16] J. G. Baker, M. Campanelli, F. Pretorius, and Y. Zlochower, Classical Quantum Gravity **24**, S25 (2007).
[17] P. Marronetti *et al.*, Classical Quantum Gravity **24**, S43 (2007).
[18] H. P. Pfeiffer *et al.*, Classical Quantum Gravity **24**, S59 (2007).
[19] U. Sperhake, V. Cardoso, F. Pretorius, E. Berti, and J. A. Gonzalez, Phys. Rev. Lett. **101**, 161101 (2008).
[20] M. Campanelli, C. O. Lousto, Y. Zlochower, and D. Merritt, Astrophys. J. **659**, L5 (2007).
[21] M. Campanelli, C. O. Lousto, Y. Zlochower, and D. Merritt, Phys. Rev. Lett. **98**, 231102 (2007).
[22] B. Krishnan, C. O. Lousto, and Y. Zlochower, Phys. Rev. D **76**, 081501 (2007).
[23] S. Dain, C. O. Lousto, and Y. Zlochower, Phys. Rev. D **78**, 024039 (2008).
[24] M. Campanelli, Classical Quantum Gravity **22**, S387 (2005).
[25] F. Herrmann, D. Shoemaker, and P. Laguna, AIP Conf. Proc. **873**, 89 (2006).
[26] J. G. Baker *et al.*, Astrophys. J. **653**, L93 (2006).
[27] C. F. Sopuerta, N. Yunes, and P. Laguna, Phys. Rev. D **74**, 124010 (2006).
[28] J. A. González, U. Sperhake, B. Brugmann, M. Hannam, and S. Husa, Phys. Rev. Lett. **98**, 091101 (2007).
[29] C. F. Sopuerta, N. Yunes, and P. Laguna, Astrophys. J. **656**, L9 (2007).
[30] F. Herrmann, I. Hinder, D. Shoemaker, and P. Laguna, AIP Conf. Proc. **873**, 89 (2006).
[31] F. Herrmann, I. Hinder, D. Shoemaker, and P. Laguna, Classical Quantum Gravity **24**, S33 (2007).
[32] F. Herrmann, I. Hinder, D. Shoemaker, P. Laguna, and R. A. Matzner, Astrophys. J. **661**, 430 (2007).
[33] M. Koppitz *et al.*, Phys. Rev. Lett. **99**, 041102 (2007).
[34] D.-I. Choi *et al.*, Phys. Rev. D **76**, 104026 (2007).
[35] J. A. González, M. D. Hannam, U. Sperhake, B. Brugmann, and S. Husa, Phys. Rev. Lett. **98**, 231101 (2007).
[36] J. G. Baker *et al.*, Astrophys. J. **668**, 1140 (2007).
[37] E. Berti *et al.*, Phys. Rev. D **76**, 064034 (2007).
[38] W. Tichy and P. Marronetti, Phys. Rev. D **76**, 061502 (2007).
[39] F. Herrmann, I. Hinder, D. M. Shoemaker, P. Laguna, and R. A. Matzner, Phys. Rev. D **76**, 084032 (2007).
[40] B. Brugmann, J. A. Gonzalez, M. Hannam, S. Husa, and U. Sperhake, Phys. Rev. D **77**, 124047 (2008).
[41] J. D. Schnittman *et al.*, Phys. Rev. D **77**, 044031 (2008).
[42] K. Holley-Bockelmann, K. Gultekin, D. Shoemaker, and N. Yunes, arXiv:0707.1334.
[43] D. Pollney *et al.*, Phys. Rev. D **76**, 124002 (2007).
[44] I. H. Redmount and M. J. Rees, Comments Astrophys. **14**, 165 (1989).
[45] D. Merritt, M. Milosavljevic, M. Favata, S. A. Hughes, and D. E. Holz, Astrophys. J. **607**, L9 (2004).
[46] A. Gualandris and D. Merritt, arXiv:0708.0771.
[47] R. C. Kapoor, Pramana **7**, 334 (1976).
[48] T. Bogdanovic, C. S. Reynolds, and M. C. Miller, arXiv: astro-ph/0703054.
[49] A. Loeb, Phys. Rev. Lett. **99**, 041103 (2007).
[50] E. W. Bonning, G. A. Shields, and S. Salviander, arXiv:0705.4263.
[51] S. Komossa, H. Zhou, and H. Lu, Astrophys. J. Lett. **678**, L81 (2008).
[52] S. Komossa and D. Merritt, Astrophys. J. **683**, L21 (2008).
[53] G. A. Shields, E. W. Bonning, and S. Salviander, arXiv:0810.2563.
[54] L. Rezzolla *et al.*, Astrophys. J. **674**, L29 (2008).
[55] U. Sperhake *et al.*, Phys. Rev. D **78**, 064069 (2008).
[56] C. O. Lousto and Y. Zlochower, Phys. Rev. D **77**, 024034 (2008).
[57] M. Campanelli, C. O. Lousto, and Y. Zlochower, Phys. Rev. D **77**, 101501(R) (2008).
[58] P. O. Mazur, arXiv:hep-th/0101012.
[59] M. Campanelli, B. Kelly, and C. O. Lousto, Phys. Rev. D **73**, 064005 (2006).
[60] J. Baker, M. Campanelli, and C. O. Lousto, Phys. Rev. D **65**, 044001 (2002).
[61] J. Baker and M. Campanelli, Phys. Rev. D **62**, 127501 (2000).
[62] O. Dreyer, B. Krishnan, D. Shoemaker, and E. Schnetter, Phys. Rev. D **67**, 024018 (2003).
[63] M. Campanelli and C. O. Lousto, Phys. Rev. D **59**, 124022 (1999).
[64] C. O. Lousto and Y. Zlochower, Phys. Rev. D **76**, 041502 (R) (2007).
[65] M. A. Scheel *et al.*, Phys. Rev. D **79**, 024003 (2009).
[66] M. Mars, Classical Quantum Gravity **16**, 2507 (1999).
[67] M. Mars, Classical Quantum Gravity **17**, 3353 (2000).
[68] B. F. Whiting, J. Math. Phys. (N.Y.) **30**, 1301 (1989).
[69] G. Dotti, R. J. Gleiser, I. F. Ranea-Sandoval, and H. Vucetich, Classical Quantum Gravity **25**, 245012 (2008).
[70] H. Stephani, D. Kramer, M. MacCallum, C. Hoenselaers, and E. Herlt, *Exact Solutions to Einstein's Field Equations* (Cambridge University Press, Cambridge, England, 2003), 2nd ed., p. 701.
[71] R. A. d'Inverno and R. A. Russel-Clark, J. Math. Phys. (N.Y.) **12**, 1258 (1971).
[72] J. Carminati and R. McLenaghan, J. Math. Phys. (N.Y.) **32**, 3135 (1991).
[73] L. Gunnarsen, H. Shinkai, and K. Maeda, Classical Quantum Gravity **12**, 133 (1995).
[74] S. Chandrasekhar, *The Mathematical Theory of Black Holes* (Oxford University Press, Oxford, England, 1983).
[75] M. Abramowitz and I. Stegun, *Handbook of Mathematical Functions* (Dover, New York, 1972), 10th ed.
[76] H. Stephani, *Relativity: An Introduction to Special and General Relativity* (Cambridge University Press, Cambridge, England, 2004), 3rd ed.
[77] J. B. Griffiths and J. Podolsky, Classical Quantum Gravity **22**, 3467 (2005).
[78] C. Beetle, M. Bruni, L. M. Burko, and A. Nerozzi, Phys. Rev. D **72**, 024013 (2005).

[79] S. Brandt and B. Brügmann, Phys. Rev. Lett. **78**, 3606 (1997).
[80] M. Ansorg, B. Brügmann, and W. Tichy, Phys. Rev. D **70**, 064011 (2004).
[81] Y. Zlochower, J. G. Baker, M. Campanelli, and C. O. Lousto, Phys. Rev. D **72**, 024021 (2005).
[82] T. Nakamura, K. Oohara, and Y. Kojima, Prog. Theor. Phys. Suppl. **90**, 1 (1987).
[83] M. Shibata and T. Nakamura, Phys. Rev. D **52**, 5428 (1995).
[84] T. W. Baumgarte and S. L. Shapiro, Phys. Rev. D **59**, 024007 (1998).
[85] P. Marronetti, W. Tichy, B. Brugmann, J. Gonzalez, and U. Sperhake, Phys. Rev. D **77**, 064010 (2008).
[86] E. Schnetter, S. H. Hawley, and I. Hawke, Classical Quantum Gravity **21**, 1465 (2004).
[87] M. Alcubierre, B. Brügmann, P. Diener, M. Koppitz, D. Pollney, E. Seidel, and R. Takahashi, Phys. Rev. D **67**, 084023 (2003).
[88] C. Gundlach and J. M. Martin-Garcia, Phys. Rev. D **74**, 024016 (2006).
[89] J. Thornburg, Classical Quantum Gravity **21**, 743 (2004).
[90] M. Campanelli, C. O. Lousto, H. Nakano, and Y. Zlochower, arXiv:0808.0713 [Phys. Rev. D (to be published)].
[91] F. Echeverría, Phys. Rev. D **40**, 3194 (1989).
[92] J. Baker, M. Campanelli, C. O. Lousto, and R. Takahashi, Phys. Rev. D **65**, 124012 (2002).
[93] M. Boyle, L. Lindblom, H. Pfeiffer, M. Scheel, and L. E. Kidder, Phys. Rev. D **75**, 024006 (2007).
[94] M. Tiglio, L. E. Kidder, and S. A. Teukolsky, Classical Quantum Gravity **25**, 105022 (2008).
[95] E. Schnetter, P. Diener, E. N. Dorband, and M. Tiglio, Classical Quantum Gravity **23**, S553 (2006).
[96] B. Zink, E. Schnetter, and M. Tiglio, Phys. Rev. D **77**, 103015 (2008).